COUPLING OF WALL-SLIP AND HIGH-VELOCITY FLOW FOR DETERMINATION OF GAS PERMEABILITY

E. Skjetne and J. S. Gudmundsson,
Department of Petroleum Engineering and Applied Geophysics,
Norwegian Institute of Technology, University of Trondheim.

Abstract

Wall-slip in the high velocity flow regime has traditionally been accounted for by correcting the permeability and not the inertial resistance. A recent theory for gas flow includes a coupling between wall-slip velocity and high-velocity pressure loss. Flow experiments were done on a short sample of low permeability. Models for uncoupled and coupled wall-slip and high-velocity flow were compared to experimental results. It was found that there is a significant coupling effect which is described by the new theory.

Introduction

Determination of the permeability of cores by low pressure and high-velocity flow of gas requires corrections to Darcy's law due to two physical effects: wall-slip and inertia. These effects are included by two separate corrections (Ham et al. 1972, Jones 1987, Goggin et al. 1988, Tiss and Evans 1989, Noman and Kalam 1990). The wall slip effect is taken into account by the Klinkenberg correction of the absolute permeability and the inertia by replacing Darcy's law by the Forchheimer equation (Firoozabadi and Katz 1979, Firoozabadi et al. 1995). A stringent model for uncoupled wall-slip and high-velocity flow, called Model A, was derived by Jones (1995).

Recently, combined wall-slip and inertial gas flow has been studied (Skjetne and Gudmundsson 1993, 1995). Models were derived from the Navier-Stokes equations in which there is a close relationship between local wall-slip velocity and the viscous force. The models show that wall-slip and inertial effects are coupled. The latter model, called Model B, is more stringent than the former and is derived in the framework of flow in spatially periodic porous media. In the present work, Model A and Model B are tested against flow experiments on a tight sandstone.

Klinkenberg (1941) modeled wall-slip, low-velocity flow in an idealized porous medium consisting of capillaries of the same radius and random orientation, and found that the gas permeability k_g was related to the liquid permeability k_l by

$$k_g = k_l \left(1 + \frac{b}{p}\right), \tag{1}$$

where p is the pressure and b is the Klinkenberg coefficient which depends on gas properties and is inversely proportional to the radius of the capillaries. Klinkenberg (1941) proposed that wall-slip flow in natural porous media could be modeled by taking b as an undefined parameter. b is found from a Klinkenberg plot, which is a linear fit to the mean gas permeability $k_g(p_m)$ versus inverse mean pressure $1/p_m$.

For high-velocity laminar flow in natural porous media, the irregular flow paths induce a strong coupling between inertial, viscous and pressure forces, resulting in a pressure loss that is larger than proportional to velocity. Inertial flow effects are usually accounted for by the Forchheimer equation (Forchheimer 1901)

$$-\frac{dp}{dx} = \frac{\mu}{k}u + \beta \rho u^2, \tag{2}$$

where μ is viscosity, k is permeability, β is inertial resistance, ρ is density, u is velocity and x is the coordinate in the flow direction. For $\beta = 0$, the Forchheimer equation is reduced to Darcy's law.

Uncoupled Wall-Slip and High-Velocity Flow

Model A for uncoupled wall-slip and high-velocity flow was obtained by Jones (1995) by replacing k in Eq. (2) by $k_g(p)$ and then integrating over the core,

$$\frac{p_1^2 - p_2^2}{2\,Z\,R\,T\,L} = \frac{\frac{\mu}{k_l} q (1 + Fh)}{1 + \frac{b}{p_m(1+Fh)} \left(1 - \frac{b}{p_1 - p_2} \frac{Fh}{1+Fh} \ln \frac{p_1(1+\frac{b}{p_1}\frac{Fh}{1+Fh})}{p_2(1+\frac{b}{p_2}\frac{Fh}{1+Fh})}\right)} \tag{3}$$

$$\approx \frac{\mu}{k_l(1 + \frac{b}{p_m})} q + \beta q^2 \tag{4}$$

where L is the length of the core, p_1 and p_2 are inlet and outlet pressures and q is the mass flux

$$q = \rho u. \tag{5}$$

To obtain Eq. (3), the real gas law was used

$$p = Z \rho R T, \tag{6}$$

where Z is the compressibility factor, R is the gas constant and T is the temperature. A Forchheimer number Fh has been introduced in Eq. (3) as the ratio of non-linear to linear pressure loss for liquid flow

$$Fh = \frac{k_l \beta q}{\mu} \tag{7}$$

For large pressure losses, the pressure dependence in the physical properties should also be integrated. However, a good approximation is to use the physical properties at mean pressure, i.e. replacing Z and μ by Z_m and μ_m.

Coupled Wall-Slip and High-Velocity Flow

Skjetne and Gudmundsson (1995) derived the following Model B for coupled wall-slip in the high-velocity flow

$$\frac{(p_1^2 - p_2^2)}{2\,Z\,R\,T\,L} = \frac{\frac{\mu}{k_l} q\,(1 + Fh)}{\left[1 + \frac{b}{p_m}(1 + 2Fh)\right][1 - C]} \tag{8}$$

$$\approx \frac{\frac{\mu}{k_l} q\,(1 + Fh)}{1 + \frac{b}{p_m}(1 + 2Fh)} \tag{9}$$

where

$$C = \frac{b^2 Fh(1 + Fh)}{2p_m(p_1 - p_2)\left[1 + \frac{b}{p_m}(1 + 2Fh)\right]} \ln(D), \tag{10}$$

$$D = \frac{p_1^2\left[\left(1 + \frac{b}{p_1}(1 + Fh)\right)^2 + Fh(1 + Fh)\left(\frac{b}{p_1}\right)^2\right]}{p_2^2\left[\left(1 + \frac{b}{p_2}(1 + Fh)\right)^2 + Fh(1 + Fh)\left(\frac{b}{p_2}\right)^2\right]}. \tag{11}$$

C is a second order wall-slip correction term and is usually small when compared to unity, as is indicated by the approximation. b was given as the product of a gas dependent part b_g and a rock dependent part b_r

$$b = b_g b_r,\ b_g = \mu\sqrt{\pi RT/2},\ b_r = \frac{\phi R_H W}{k_l}, \tag{12}$$

where R_H is the average hydraulic radius defined by

$$R_H = \frac{\text{Total Pore Volume}}{\text{Total Pore Surface}}, \tag{13}$$

and W is a constant which is equal to unity for capillary tubes of uniform radius. $R_H W$ is an effective hydraulic radius, that is a weighted average of the hydraulic radius, where the weight is the local wall-slip velocity.

Model A and Model B can now be compared. The relative difference between the approximations of the pressure loss of Model A (Eq. (4)) and Model B (Eq. (9))

for a given set of parameters k_l, b and β can be expressed as

$$\frac{(\text{Model A})_a - (\text{Model B})_a}{(\text{Model B})_a} = \left(2 + \frac{1 + \frac{b}{p_m}(1+2Fh)}{1+Fh}\right) \frac{\frac{b}{p_m}Fh}{1+\frac{b}{p_m}} \approx 3\frac{b}{p_m}Fh. \quad (14)$$

The pressure loss is larger for Model A than for Model B. The models are identical in the limits of Darcy flow $Fh \rightarrow 0$ and no-slip flow $b/p_m \rightarrow 0$.

One way to distinguish between the two models is first to obtain b_r and k_l from a Klinkenberg plot for experiments in the low velocity regime where the two models are almost identical. Then, to carry out an experiment where the relative difference term increases monotonically and check whether the parameters fitted for Model A and Model B are consistent with b_r and k_l obtained from the Klinkenberg plot.

Experiments

The core sample used was an Obernkirchner tight and well sorted sandstone of diameter 37.9 mm and length 9.55 mm. The sample was machined in a lath to obtain parallel end faces, cleaned in methanol, and dried. The porosity was measured with a helium porosimeter.

The laboratory setup to measure pressure loss versus rate is shown in Figure 1. The measuring devices were one pressure meter for the range 0-20 barg, two differential pressure meters with variable ranges 0-0.064/0.64 bar and 0-3.0/30.0 bar and three flow meters 0-2.0 ln/min, 0-16.1 ln/min, and 0-53.66 ln/min, where [ln] is normal liter (at 273.15 K and 1.013 bar). Prior to the experiments, the flow meters were calibrated at the factory by a standard traceable to the national standard of the Dutch Weights & Measures and corrected by a third order polynomial.

The gas was nitrogen. It flowed, via a regulator, into a copper coil, made of a 3 m long copper pipe, placed in a temperature controlled water bath, kept at room temperature ($\approx 294\ K$). The temperature was measured by a Pt 100 thermometer. The function of the coil was to obtain constant gas temperature, independent of rate and a possible cooling due to the Joule-Thomson effect. Then, the gas flowed through one of the flow meters and into a piston core holder and through the core. At last, the gas was regulated out to atmospheric pressure.

Results and Discussion

Two types of experiments were carried out: low-velocity flow experiments for a Klinkenberg plot and a combined wall-slip, high-velocity flow experiment. The resulting parameters are given in Table 1. For the Klinkenberg plot, 6 series at different constant p_m, with 7 data points in each series, were carried out and

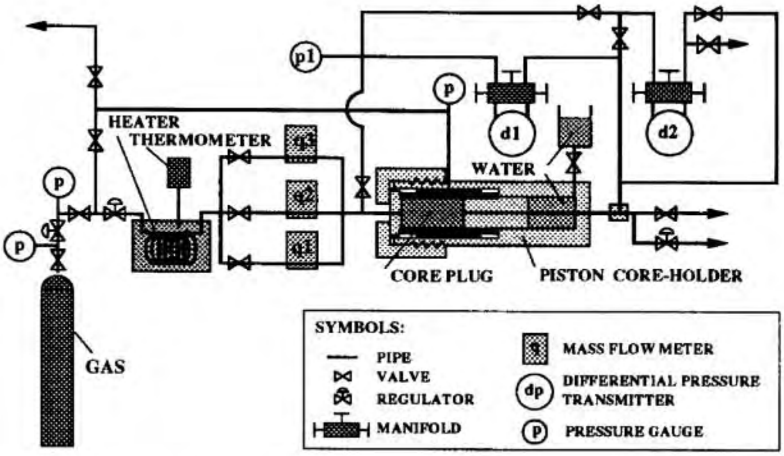

Figure 1: The main parts of the high-velocity flow setup.

Darcy's law was fitted to each series of data. A linear fit to the resulting Klinkenberg plot gave $k_l = 6.914\ 10^{-15}\, m^2$ and $b = 3.35\ 10^4\, Pa$ (Figure 2). As μ_m and T were almost constant, $b_r = 5.147\ 10^6\, 1/m$ was calculated by using Eq. (12) and μ_m and T for low p_m. The parameters obtained from the Klinkenberg plot were assumed to be the correct or "true" values of the core sample.

The effective hydraulic radius was calculated to be $R_H W = 1.77\ 10^{-7}\, m$ by using Eq. (12) with $\phi = 0.2015$ obtained from the helium porosimeter. Such a small $R_H W$ indicates that the pore network is dominated by a series coupling of small and large pores, which is consistent with the low k_l and relatively large ϕ.

Table 1: Parameters Obtained from Least Squares Fits

Model	k_l $[10^{-15}\ m^2]$	$b_r[10^6\ 1/m]$	β $[10^9\ 1/m]$	Fixed Parameters
Klinkenberg	6.914	5.147		
Model A	6.914	5.147	5.138	k_l and b_r
Model B	6.914	5.147	6.151	
Model A	5.48	48.1	6.68	
Model A, Approx.	5.81	36.3	6.4	
Model B	6.868	7.7	7.15	

A monotonic increase in Fhb/p_m was obtained from one series with 64 data points starting at $p_1 \approx p_2 \approx 10^6\, Pa$, and then reducing p_2 down to about atmospheric pressure was carried out. Model A and Model B and the approximations of the models were fitted to the data using non-linear least squares with up to 5 depen-

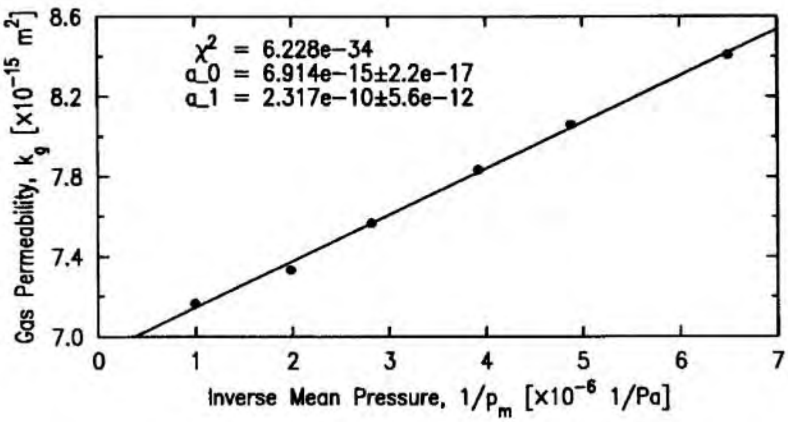

Figure 2: A Klinkenberg plot, i.e. k_g vs. $1/p_m$. The linear fit resulted in $k_l = a_0 = 6.914\ 10^{-15}\ m^2$ and $b = a_1/a_0 = 3.35\,10^4\ Pa$.

dent variables (q, p_m, p_1, p_2, and μ_m). The LHS of Eq. (3) (or Eq. (8)) was used as independent variable and as inverse weight.

First, β was fitted, while k_l and b_r were assigned the "true" values (Figure 3). The total pressure loss is the sum of the Darcy ($\beta = 0$) and the non-Darcy pressure losses which are plotted as dashed lines. The mean pressure is plotted with a scale on the right axis. Model A does not fit the trend of high-velocity data well. β is systematically too small for medium q and too large for high q. Model B fits well. β is 16 % smaller for Model A than for Model B, but the pressure loss for the highest q is largest for Model A. Model A ignores wall-slip effects on β, and compensates for this by reducing β.

Then, k_l, β, and b_r were fitted. The results are shown in Figure 4. Both models fit the data well. Compared to the "true" values, Model A underestimated k_l by 21 % and overestimated b_r by 935 %, whereas Model B underestimated k_l with 6.7 % and overestimated b_r 50 %. Some of this discrepancy may be explained by that an increase in b_r is partly compensated for by a decrease in k_l and an increase in β, so that there is a large region in parameter space that fits the data well.

This may explain the discrepancy of Model B, but the discrepancy of Model A is too large for both k_l and b_r to justify that Model A is still valid. Given that Model B is valid, we expect that Model A compensates for no wall-slip correction of β by using a b_r that is larger than the "true" value and compensates for the too large b_r at small q by reducing k_l. Thus, the discrepancy of Model A is explained by the effects accounted for in Model B.

The approximations of the models resulted in the same parameters as for the

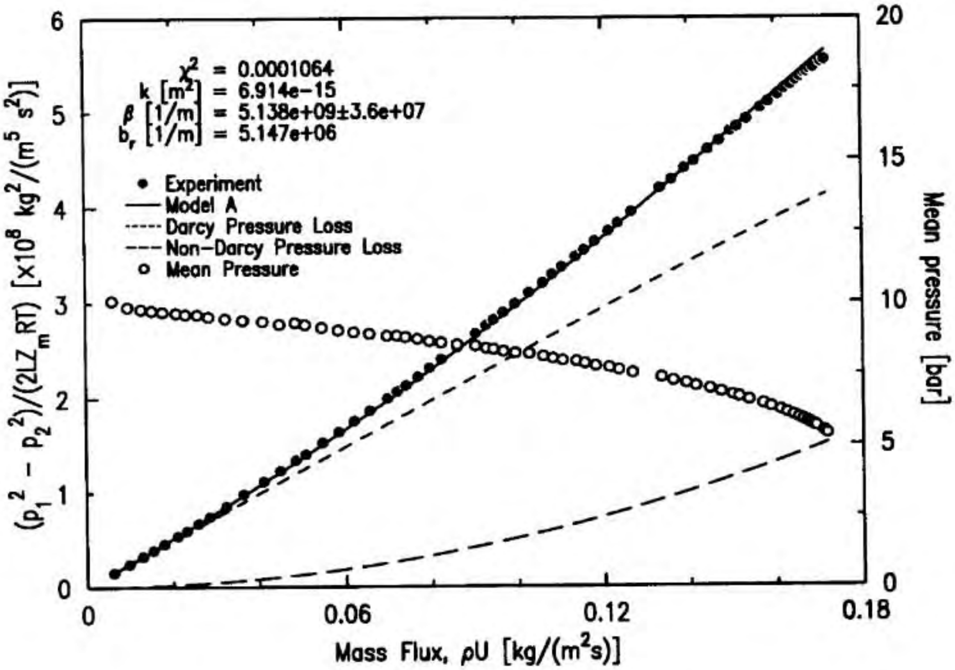

(a)

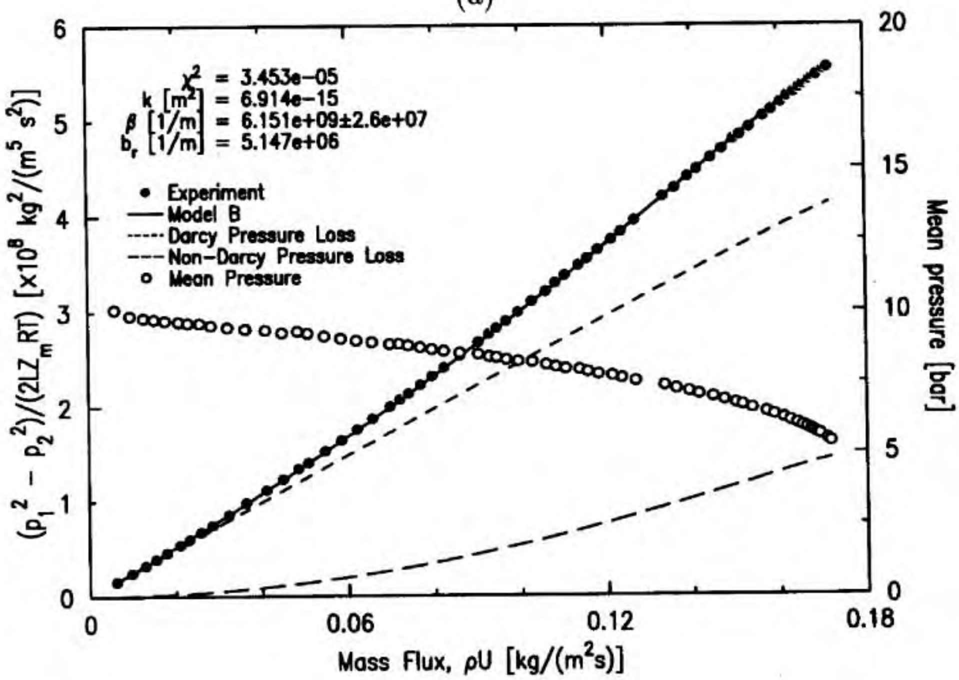

(b)

Figure 3: Model A (a) and Model (b) with β fitted to the experimental data. k_l and b_r was taken from the fit in the Klinkenberg plot Figure 2.

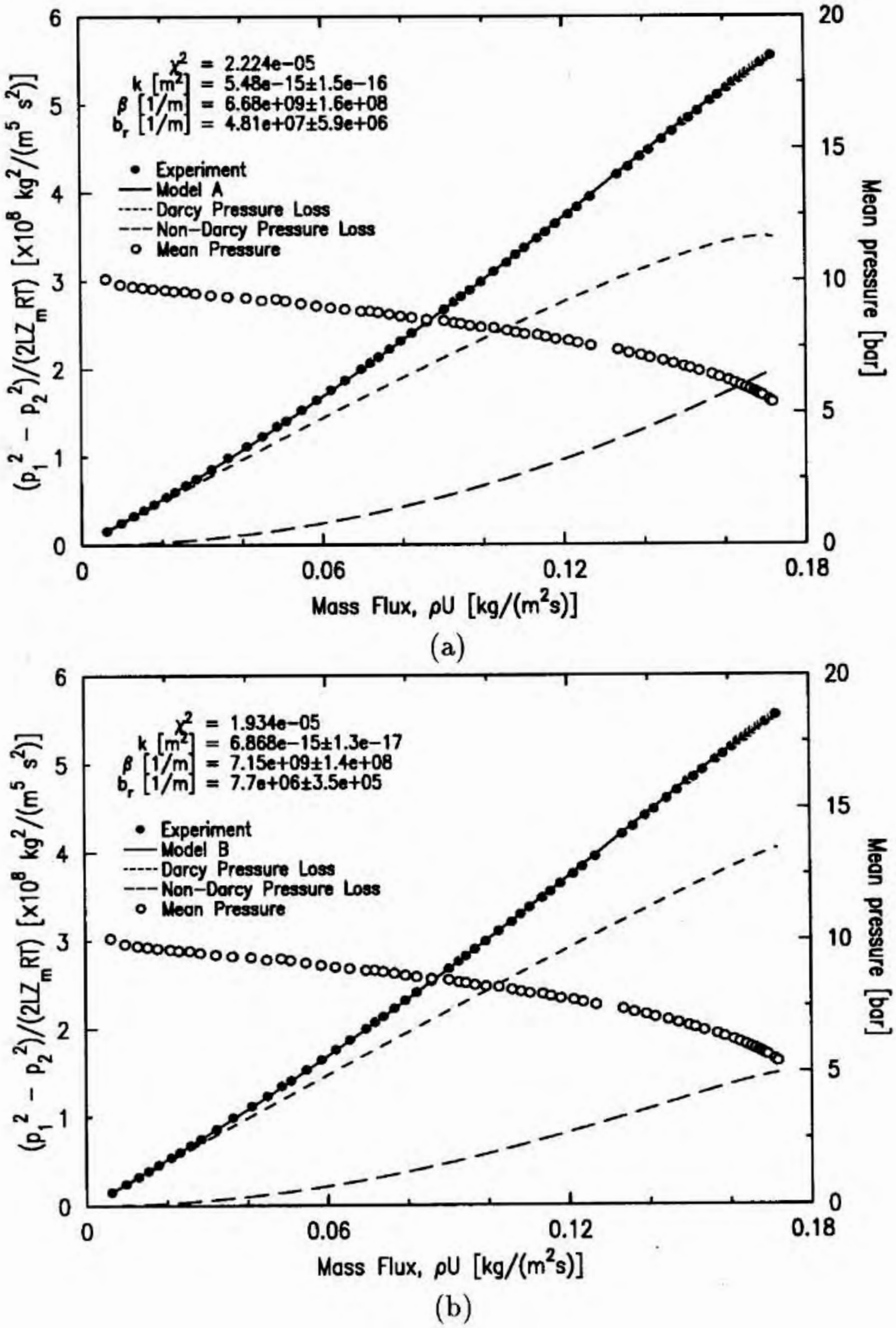

Figure 4: Model A (a) and Model B (b) with k_l, β, and b_r fitted to experimental data.

models, except for the approximation of Model A fitting all parameters. Since our experiment had both high-velocity and significant wall-slip, it is likely that the approximation of Model B is generally very good. Summing up the discussion, Model A is less valid than Model B for wall-slip, high-velocity flow, and the approximation of Model B gives the same results as the full Model B.

Conclusions

1. It has been shown experimentally that there is a significant coupling between wall-slip and high-velocity gas flow. This coupling can be described by the theory of Skjetne and Gudmundsson (1995).
2. Neglecting the wall-slip/high-velocity coupling resulted in a permeability underestimated by 20 % and a Klinkenberg factor overestimated by an order of magnitude.
3. The use of Eq. (9) for analysis of wall-slip high-velocity flow is recommended.

Acknowledgments

We are grateful to Hilde Lunde for preliminary experimental work and Øyvind Sylta for providing core samples. Financial support was received from the Research Council of Norway through the non-Darcy Flow project (426.91/063) in the PROPETRO Program.

Nomenclature

b	=	Klinkenberg Coefficient $[Pa]$.
b_g	=	Gas Dependent Part of the Klinkenberg Coefficient $[Pa\ m]$.
b_r	=	Rock Dependent Part of the Klinkenberg Coefficient $[1/m]$.
C	=	Second Order Wall-Slip Correction Term in Model B.
D	=	Term in C.
Fh	=	Forchheimer Number.
k	=	Permeability $[m^2]$.
k_g	=	Gas Permeability at a Given Pressure $[m^2]$.
k_l	=	Liquid Permeability $[m^2]$.
L	=	Core Length $[m]$.
p	=	Pressure $[Pa]$.
R	=	Gas Constant $[m^2/(s^2K)]$.
R_H	=	Total Hydraulic Radius $[m]$.
u	=	Volume Averaged Velocity (Seepage Velocity) $[m/s]$.
T	=	Temperature $[K]$.
x	=	Coordinate Along the Core $[m]$.
W	=	Weight Factor for Hydraulic Radius.
Z	=	Compressibility Factor.

β = Inertial Resistance or High-Velocity Flow Coefficient $[1/m]$.
μ = Viscosity $[Pa\ s]$.
ρ = Density $[kg/m^3]$.
ϕ = Porosity.
m = Subscript for Arithmetic Mean.
1, 2 = Subscripts for Inlet and Outlet.

References

Firoozabadi, A. and Katz, D. L. (1979), 'An analysis of high-velocity gas flow through porous media', *Journal of Petroleum Technology* pp. 211–216.

Firoozabadi, A., Thomas, L. K. and Todd, B. (1995), 'High-velocity flow in porous media', *SPE Reservoir Engineering* pp. 149–152.

Forchheimer, P. (1901), 'Wasserbewegnung durch Boden', *Z. d. V. deutch. Ing.* **45**(50), 1781–1788.

Goggin, D. J., Thrasher, R. L. and Lake, L. W. (1988), 'A theoretical and experimental analysis of minipermeameter response. including gas slippage and high velocity flow effects', *In Situ* **12**(1 and 2), 79–116.

Ham, J. D., Brill, J. P. and Eilerts, C. K. (1972), 'Parameters for computing pressure gradients and the equilibrium saturation of gas-condensate fluids flowing in sandstones', *SPE* pp. 203–215.

Jones, S. C. (1987), 'Using the inertial coefficient, β, to characterize heterogeneity in reservoir rock,', *SPE 16949* pp. 165–175.

Jones, S. C. (1995), personal communication.

Klinkenberg, L. J. (1941), 'The permeability of porous media to liquids and gases', *Drill. and Prod. Prac. , API* pp. 200–213.

Noman, R. and Kalam, M. Z. (1990), Transistion from laminar flow to non-Darcy flow of gas in porous media, *in* P. F. Worthington, ed., 'Advances in Core Evaluation', Sci. Publ., New York, pp. 447–462.

Skjetne, E. and Gudmundsson, J. S. (1993), Model for wall-slip in the Darcy and Forchheimer gas flow regimes, *in* 'Third Lerkendal Petroleum Engineering Workshop, January 20–21', Norwegian Institute of Technology, Tapir Publishers, Trondheim, pp. 111–122.

Skjetne, E. and Gudmundsson, J. S. (1995), Model for wall-slip gas flow in porous media, In Preparation.

Tiss, M. and Evans, R. D. (1989), 'Measurement and correlation of non-Darcy flow coefficient in consolidated porous media', *J. Pet. Sci. Eng.* **3**, 19–33.